Journal of Materials Chemistry B

PAPER

View Article Online
View Journal | View Issue

Cite this: J. Mater. Chem. B, 2015, 3, 2109

Use of nucleic acids anchor system to reveal apoferritin modification by cadmium telluride nanoparticles

Jiri Kudr,[ab] Lukas Nejdl,[ab] Sylvie Skalickova,[a] Michal Zurek,[b] Vedran Milosavljevic,[ab] Renata Kensova,[ab] Branislav Ruttkay-Nedecky,[ab] Pavel Kopel,[ab] David Hynek,[ab] Marie Novotna,[ab] Vojtech Adam[ab] and Rene Kizek*[ab]

Received 11th August 2014
Accepted 15th January 2015

DOI: 10.1039/c4tb01336k

www.rsc.org/MaterialsB

The aim of this study was to synthesize cadmium telluride nanoparticles (CdTe NPs) modified apoferritin, and examine if apoferritin is able to accommodate CdTe NPs. Primarily, the thermostability of horse spleen apoferritin was tested and it's unfolding at 70 °C was observed. Cadmium telluride nanoparticles (CdTe NPs) were synthesized both within apoferritin protein cage and on its surface. The thermal treatment of apoferritin with CdTe NPs resulted in the aggregation of cores, which was indicated by changes in the absorption spectra and the shape of apoferritin tryptophan fluorescence. The apoferritin modified with CdTe NPs was additionally modified with gold nanoparticles and attached to magnetic particles *via* oligonucleotide using gold affinity to thiol group. This anchor system was used to separate the construct using external magnetic field and to analyse the molecules attached to apoferritin.

1. Introduction

Nanoparticles have been attracting a great attention due to their wide potential of application,[1] where their different shapes, sizes and compositions enhance a possibility of broad range of their use.[2–4] For nanotechnology and biotechnology applications, there is a strong demand on uniformity of nanoparticles properties. However, there are still technical challenges regarding the preparation of nanoparticles with homogeneous size distribution.[5]

Various nanoparticles fabrication methods have been reported.[6–8] It was shown that biomolecules, such as protein cages or viruses, can serve as a template for the synthesis of nanoparticles.[9,10] The cage-like proteins are able to bio-mineralize inorganic materials; moreover, they can be used as a spatially restricted chemical chamber (nanoreactor). Among all protein cages, apoferritin is favoured for its remarkably stable structure under various acidity and temperature.[11,12] Apoferritin is an iron storage protein, which is ubiquitous in animals. It is composed of 24 polypeptide subunits. These heavy and light subunits self-assemble into a hollow protein sphere with outer and inner diameters of 12 and 8 nm, respectively.[13] Horse-spleen apoferritin is composed of nearly of 90% of L-subunit (one tryptophan per L and H subunit at the same position of polypeptide chain). Specific threefold channels at the interface of the subunits are responsible for the flow of positive ions to the hollow core. In recent research, apoferritin has been used to synthesize various metal nanoparticles and semiconductor nanocrystals.[14–20] In these cases, aspartate and glutamate on the inner surface proved to promote the formation of nanoparticles.[17] In addition, apoferritin is used in many biomedical applications.[21–23]

Magnetic particles have important applications in biochemistry and analytical chemistry such as analyte preconcentration, separation and identification.[24–26] The target molecule can be recognized by specific magnetic particle surface modification and the magnetic force enables the separation of adsorbed target molecule from a complex sample.[27,28] The modification of magnetic particles with oligonucleotide probe is broadly used for biosensors fabrication and medical applications due to their unique biorecognition properties based on the ability to hybridize target sequence and to eliminate non-specific adsorption.[29–33]

As it was mentioned above protein cages, including apoferritin, are broadly used in the field of material science. Therefore, the aim of this study was to synthesize CdTe NPs modified apoferritin, and examine if apoferritin is able to accommodate CdTe NPs. Moreover, we designed the anchor system based on modified magnetic particles to prove apoferritin modification by CdTe NPs. The advantage of the proposed system is not only in the synthesis of nanoparticles within the apoferritin cage but also in the possibility to purify this nanoreactor from the unreacted components of the synthesis, as well as to transfer it to the desired location by

[a]Department of Chemistry and Biochemistry, Faculty of Agronomy, Mendel University in Brno, Zemedelska 1, CZ-613 00 Brno, Czech Republic, European Union. E-mail: kizek@sci.muni.cz; Fax: +420-5-4521-2044; Tel: +420-5-4513-3350

[b]Central European Institute of Technology, Brno University of Technology, Technicka 3058/10, CZ-616 00 Brno, Czech Republic, European Union

external magnetic field manipulation due to the conjugation with magnetic field responsive particles.

2. Material and methods

2.1. Chemicals

Water, cadmium acetate dihydrate, sodium tellurite, sodium borohydride and other chemicals were purchased from Sigma-Aldrich (St. Louis, USA) in ACS purity (chemicals meet the specifications of the American Chemical Society), unless noted otherwise. Apoferritin from equine spleen (0.2 μm filtered) and the oligonucleotides were also purchased from Sigma-Aldrich (St. Louis, USA). Magnetic particles Dynabeads Oligo$(dT)_{25}$ were bought from Thermo Fisher Scientific (Waltham, USA). pH was measured with a pH meter WTW (inoLab, Weilheim, Germany).

2.2. Sample preparation

The apoferritin with CdTe NPs (ApoCdTe NPs) was prepared as follows. The horse spleen apoferritin (20 μl, 7.3 μg μl^{-1}) was pipetted into water (300 μl). Then, cadmium acetate (20 μl, 20 mM) and ammonium (4.5 μl, 1 M) were added. After shaking (30 min, 37 °C, 500 rpm) on a thermomixer (Eppendorf, Hamburg, Germany), and then sodium tellurite (3.75 μl, 20 mM) was added to the solution (pH 9.5). To obtain the ApoCdTe NPs sample, sodium borohydride was added to the solution. The control sample (CdTe NPs sample) was prepared in the same way by adding 20 μl of water, instead of apoferritin. The water solution of apoferritin (0.4 mg ml^{-1}) was used to compare the ApoCdTe NPs and apoferritin fluorescence and absorption. After incubation (20 h, 60 °C, 500 rpm) on a thermomixer (Eppendorf, Germany), all the samples were filtered using the Amicon Ultra-0.5 ml Centrifugal Filters with 50 kDa cut-off (Merck Millipore, Billerica, USA) according to the manufacturer instructions.

2.3. Preparation of gold nanoparticles (Au NPs)

Gold nanoparticles were prepared using citrate method at room temperature as reported elsewhere.[34,35] Briefly, an aqueous solution of sodium citrate (0.5 ml, 40 mM) was added to a solution of $HAuCl_4 \cdot 3H_2O$ (10 ml, 1 mM). The colour of the solution slowly changed from yellow to violet. The mixture was stirred overnight. The smallest Au NPs from the top layer of the flask were used for apoferritin modification according to the following protocol. The ApoCdTe NPs, CdTe NPs and apoferritin sample (100 μl) were mixed with the Au NPs (10 μl) and incubated (24 h, 500 rpm, 37 °C) in a thermomixer (Eppendorf, Germany).

2.4. Preparation of anchor system

Buffers used for the isolation step were phosphate buffer I (pH 6.5, 0.1 M NaCl, 0.05 M Na_2HPO_4, and 0.05 M NaH_2PO_4), phosphate buffer II (0.2 M NaCl, 0.1 M Na_2HPO_4, and 0.1 M NaH_2PO_4) and hybridization buffer (100 mM Na_2HPO_4, 100 mM NaH_2PO_4, 0.5 M NaCl, 0.6 M guanidium thiocyanate, and 0.15 M trizma base, pH was adjusted to 7.5 using HCl). 10 μl of the resuspended magnetic particles were placed on the magnetic stand and washed 3-times with phosphate buffer I (100 μl). The magnetic particles were resuspended in the solution containing hybridization buffer (10 μl) and oligonucleotide with polyadenine terminus (10 μl, 100 μg ml^{-1}, 5′-TCTGCATTCCA GATGGGAGCATGAGATGAAAAA). Subsequently, this solution was incubated (30 min, 500 rpm, 37 °C) on thermomixer (Eppendorf, Germany) and the particles were washed with phosphate buffer I (100 μl) in order to remove unattached oligonucleotide. The particles were then resuspended in the solution containing hybridization buffer (10 μl) and thiolated oligonucleotide (10 μl, 100 μg ml^{-1}, 5′-CATCTCATGCTCC CATCTGGAATGCAGA–SH). After incubation (30 min, 500 rpm, 37 °C), the unbounded oligonucleotides were washed away. The product was the modified magnetic particles without any fluid. The prepared construct was used to anchor the gold modified ApoCdTe NPs, apoferritin and CdTe NPs samples.

The samples with different ApoCdTe NPs concentrations and modified by Au NPs were obtained by diluting the stock solution of ApoCdTe NPs with water in different ratios (undiluted ApoCdTe NPs stock solution, 1 : 1, 1 : 3, 1 : 7, 1 : 15 and 1 : 39). The gold modified apoferritin sample (5 μl) and CdTe NPs sample mixed with Au NPs (5 μl) were also mixed with water (35 μl) and used as controls for cadmium detection after separation conducted by the anchor system. In addition, these samples (40 μl) were mixed with the prepared modified magnetic particles and incubated (1 h, 25 °C, 500 rpm). Subsequently, the magnetic particles were washed with phosphate buffer I (100 μl), and phosphate buffer II was added (10 μl) in order to split the hybridized oligonucleotides. The magnetic particles were immobilized by the magnetic field and the supernatants were analysed using atomic absorption spectrometry (AAS).

2.5. Instrumentation

Absorption and fluorescence spectra were measured using an Infinite 200 PRO multimode reader with top heating (Tecan, Männedorf, Switzerland). Gel electrophoresis was performed using a PowerPac Universal Power Supply (Bio-Rad, Hercules, USA). Average current levels were obtained using a Scanning electrochemical microscope 920C (CH Instruments, Austin, USA). Spectro Xepos (Spectro Analytical Instruments, Kleve, Germany) was used to measure X-ray fluorescence spectra. The determination of cadmium was carried out on a 280Z Agilent Technologies atomic absorption spectrometer (Agilent, Santa Clara, USA) with electrothermal atomization and Zeeman background correction. Average particle size and size distribution were determined by quasielastic laser light scattering with Malvern zetasizer Nano-ZS (Malvern Instruments Ltd., Worcestershire, U.K.).

2.6. Apoferritin thermostability

The unfolding of apoferritin was monitored spectrophotometrically using a computer-controlled Peltier thermostat (Labortechnik, Wasserburg, Germany). The sample (35 μg ml^{-1}) was incubated at different temperatures for 5 min, and thereafter the absorbance was measured at 230 nm. Changes in sample

absorbance were recorded using a spectrophotometer Specord S600 with a diode detector (Analytik Jena, Jena, Germany). The thermostability of apoferritin was also tested using gel electrophoresis. The solution of apoferritin (35 μg ml^{-1}) was shaken (500 rpm) and heated with a thermomixer. The samples (10 μl) were removed from the solution during heating when the temperature reached 30, 35, 40, 45, 50, 55, 60, 65, 70 and 75 °C for 5 minutes. These samples were further analysed by native (non-denaturing) polyacrylamide gel electrophoresis (native-PAGE).

2.7. Non-denaturing polyacrylamide gel electrophoresis

The samples were analysed in 6% non-denaturing PAGE in 60 mM 4-(2-hydroxyethyl)-1-piperazineethanesulfonic acid and 40 mM imidazole pH 7.4 buffer as described by Kilic *et al.*[36] Briefly, the samples (10 μl) were mixed with 2 μl of 30% glycerol. The gels (2.4 ml of acrylamide/bis-acrylamide 30% solution, 9.6 ml of running buffer, 9.96 μl of *N*,*N*,*N*′,*N*′-tetramethylethylenediamine and 60 μl of ammonium persulfate) were run at 10 mA for 2 hours (30 minutes for apoferritin thermostability experiment) and were stained with Coomassie Brilliant Blue R stain.

2.8. The scanning electrochemical microscope measurements

Scanning electrochemical microscope (SECM) consisted of 100 mm measuring platinum disc probe electrode with a potential of +0.2 V. During the scanning, particles were attached to the conducting substrate plate coated with gold *via* magnetic force from neodymium magnet. The working distance of the platinum measuring electrode was set at 20 μm above the surface. The mixture consisted of 5% ferrocene in methanol mixed in 1 : 1 ratio with 0.05% KCl with water (v/v).

2.9. Stern–Volmer constant

Fluorescence spectra (excitation wavelength 400 nm) of CdTe NPs (emission wavelength 600 nm) QDs without any capping agent (50 μl) were measured in the presence of 0, 0.3, 0.6, 0.8, 1.1 and 1.4 μM of apoferritin (5 μl) and also at different temperatures (20, 25, 30, 35 and 40 °C). The CdTe NPs fluorescence quenching by apoferritin can be described by Stern–Volmer equation:

$$\frac{F_0}{F} = 1 + k_q\tau_0[Q] = 1 + K_{SV}[Q]$$

where F_0 and F are fluorescence intensities of CdTe NPs in the absence and presence of apoferritin quencher, respectively, k_q is biomolecular quenching constant, τ_0 is the lifetime of the fluorophore without quencher, [Q] is the concentration of the quencher and K_{SV} is the Stern–Volmer quenching constant.[37] The quenching constant K_{SV} was calculated by the linear regression of a plot of $(F_0 - F)/F$ against [Q].[38]

3. Results and discussion

3.1. The synthesis of CdTe NPs within apoferritin

The H subunits (represents 10–15% of horse spleen apoferritin) include the ferroxidase centre, which is responsible for the oxidation of ferrous oxide to ferric oxide and prevents free radicals production. Apoferritin cavity *in vivo* was able to accommodate 4000 iron atoms stored as a mineral ferrihydrite. The hydrophobic fourfold channels represent large energy barrier for divalent and monovalent ions uptake.[39] Apart from that, the hydrophylic threefold channels transferred monovalent and divalent ions into the apoferritin cavity. This ability was broadly used for nanoparticle synthesis within the cavity. As it was previously proved, the apoferritin cavity was able to accommodate several metal ions and inorganic molecules.[14,15,40] From these, cadmium ions were used for ferritin and apoferritin crystallization due to its large coordination numbers,[41] and were also able to bridge the otherwise repulsive carboxyl groups of opposing aspartate and glutamine side chains.[42]

Protein contains three intrinsic fluorophores: phenylalanine, tyrosine and tryptophan, which are also responsible for protein absorption in the UV-region. Tryptophan has longer excitation and emission wavelengths and good quantum yield. Due to the fact that phenylalanine has very low quantum yield and tyrosine is often totally quenched when is located near amino or carboxyl group, protein intrinsic fluorescence mostly arises from tryptophan (its indole ring).[37] Changes in the tryptophan fluorescence intensity, band shape, wavelength maximum and fluorescence lifetime depend on the tryptophan local environment and are used in various applications such as substrate binding or quencher accessibility.[38,43–45] Both, the H and L-chains of apoferritin contain single tryptophan residue, thus 24 tryptophan residues are presented within apoferritin. Therefore, we monitored apoferritin emission spectra after excitation at 230 nm and observed the changes during the sample preparations.

The preparation of ApoCdTe NPs (apoferritin modified with CdTe NPs) is schematically depicted in Fig. 1A. More precisely, ammonium (4.5 μl, 1 M) and cadmium acetate (20 μl, 20 mM) were added to apoferritin solution (0.4 mg ml^{-1}). Cadmium ions were stabilized by ammonium ions and created positively charged tetraminecadmium ions, which were partly transported to the apoferritin cavity.[46] Then, sodium tellurite (3.75 μl, 20 mM) was added and the tellurite ions were reduced to telluride by the addition of sodium borohydride, which resulted in CdTe cores formation. Subsequent heating was applied to allow CdTe cores to aggregate.

The individual steps of ApoCdTe NPs synthesis were monitored using UV-Vis and fluorescence spectroscopy to confirm the CdTe NPs creation. The absorption (230–800 nm) and fluorescence spectra (280–480 nm) were measured and compared with two control samples as (i) CdTe NPs solution without any capping agent and apoferritin (CdTe NPs sample), and (ii) apoferritin water solution. The characteristic absorption peak of protein (apoferritin) was observed at 280 nm in the cases of apoferritin solution with cadmium and tellurite ions

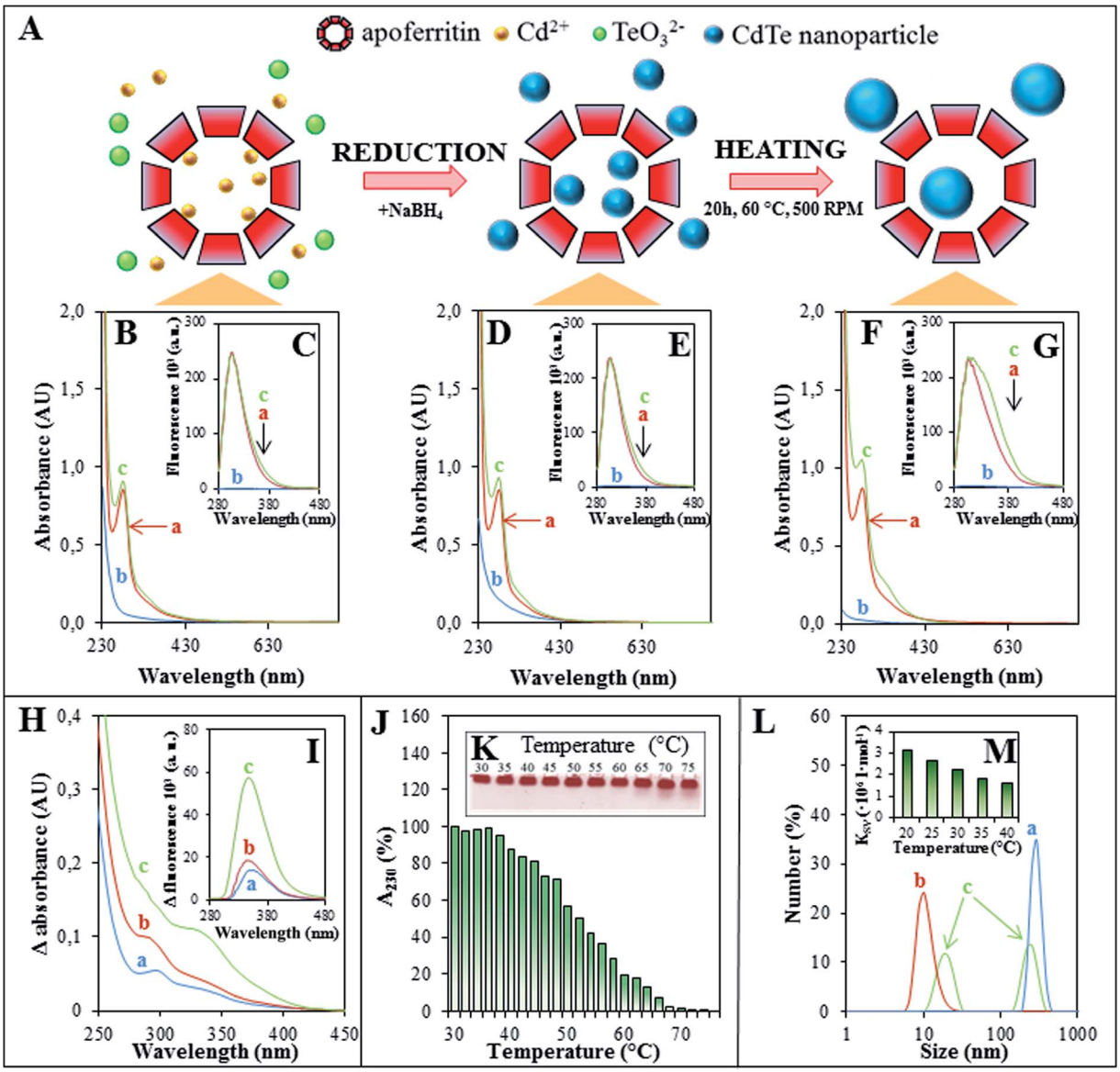

Fig. 1 Individual steps of CdTe NPs synthesis within apoferritin (ApoCdTe NPs) and their characterization. (A) The scheme of the ApoCdTe NPs synthesis, which was monitored using UV-vis spectrometry and fluorescence spectroscopy and compared with the control samples. The absorption and fluorescence spectra of (a) apoferritin solution, (b) cadmium acetate, ammonium and sodium tellurite water solution and (c) same mixture with addition of apoferritin were measured (B and C) before reduction step, (D and E) after reduction and (F and G) after heating. To highlight the differences between ApoCdTe NPs and apoferritin sample the differential (H) absorption and (I) fluorescence spectra (a) before reduction, (b) after reduction and (c) after incubation were calculated. (J) To encourage CdTe creation heating is required, thus apoferritin thermostability was determined. The absorbance of apoferritin solution at 230 nm during the heating depicted as percentages of decrease and (K) the native PAGE of heated apoferritin solution to particular temperature. (L) The size distribution of (a) CdTe colloids, (b) apoferritin in its spherical state and (c) particles presented within ApoCdTe NPs sample. (M) Stern–Volmers K_{SV} constants were determined to elucidate the interaction mechanism between CdTe NPs by apoferritin at different temperatures.

($A_{280} = 0.91$ AU) and apoferritin solution ($A_{280} = 0.86$ AU) before the addition of $NaBH_4$. No absorption peak was observed in the case of cadmium and tellurite ions solution (Fig. 1B). The fluorescence spectra of all three samples were also measured (Fig. 1C). The emission peaks of apoferritin and apoferritin in the presence of ions were observed at 308 nm. The sample with cadmium and tellurite ions without apoferritin exhibited emission spectra with no peak. In comparison to the sample of ions before the addition of reducing agent, the absorption maximum of reduced sample increased in the range from 246 nm to 450 nm due to CdTe cores creation (Fig. 1D), which is in good agreement with Han *et al.*[47] The absorption spectra of ApoCdTe NPs and apoferritin sample remained nearly the same after reduction process. The emission of ApoCdTe NPs and apoferritin samples were lowered by 4% and 3% respectively, compared to the unreduced samples (Fig. 1E). The fluorescence measurement of CdTe NPs sample immediately after reduction revealed no emission peak (excitation wavelength 230 nm), but

emission maxima was observed at 584 nm when excited at 400 nm (not shown). We assume that the presence of CdTe quantum dots in the solution was responsible for this emission maximum. In the next step, the samples were heated (20 h, 60 °C, 500 rpm) to encourage the aggregation of CdTe NPs according to Khalavka *et al.*[48] The measurement of samples absorption spectra after the heating step resulted in the increase of ApoCdTe NPs local maxima at 280 nm by 14% (compared with reduced ApoCdTe NPs sample) and the formation of local maxima at 330 nm, although the absorption spectra of apoferritin sample remained nearly the same (Fig. 1F). The similar absorption spectra of nanoparticle within apoferritin were reported for Pd and Cd.[16,49] Strong decrease in CdTe NPs sample absorption at UV wavelengths was detected after heating and we assume that this is the result of bulk CdTe colloids precipitation (Fig. 1F). Although, the fluorescence of apoferritin and ApoCdTe NPs sample with the maxima at 306 nm remained the same after incubation, the peak width changed (Fig. 1G). The emission of CdTe NPs was not observed and the mechanism of quenching is discussed afterwards. Xiao *et al.* determined the interaction of CdTe quantum dots stabilized by mercapropropionic acid with the human serum albumin by the decrease in albumin fluorescence intensity, however quantum dot properties are strongly affected by the capping agent.[50] Peak width at half height of ApoCdTe NPs (calculated as a distance from the front slope of the peak to the back slope of the peak measured at 50% of the maximum peak height) increased by 54% in comparison with the emission peak before heating and also increased by 30% in the case of apoferritin solution. After the heating, no emission peak of CdTe NPs sample was observed when excited at 230 nm and the emission peak also disappeared when excited at 400 nm (not shown). Without any capping agent, heating of quantum dots resulted in their aggregation.

We also calculated the difference spectra. The absorption and fluorescence spectra of apoferritin solution in a particular synthesis step were subtracted from the spectra of ApoCdTe NPs sample. The differential absorption spectra highlighted the differences between samples at 300 nm before and after reduction step and the local maxima increase at 330 nm (Fig. 1H). The heating of ApoCdTe NPs sample resulted in the difference fluorescence maxima evolving. The differential fluorescence spectra revealed the increasing peak at 350 nm (Fig. 1I). The difference emission of heated ApoCdTe NPs and heated apoferritin increased 3-times in comparison with difference emission of the unheated samples.

In addition, the thermostability of apoferritin spherical structure was examined using UV-Vis spectrophotometry and gel electrophoresis. UV-Vis absorbance measurement is a simple method used to examine the structural changes and formation of complexes.[33,51,52] The protein absorption spectra showed the peak at 280 nm due to the absorption of aromatic side chains of phenylalanine, tyrosine, and due to disulphide bonds, which are responsible for the dimerization of apoferritin H-chains, and mostly by tryptophan.[53] The tryptophan and tyrosine content in various proteins remains constant, and therefore this wavelength is commonly used to determine protein concentration in a reagentless nondestructive way. External conditions like temperature, pH and ionic strength cause changes in the protein conformation, which results in the change of amino acids exposure to the solvent and the absorption spectra.[54–57] Although the UV absorption spectra of proteins show slopes only at app. 230 nm, according to Liu *et al.*,[58] it can be used as a convenient structural probe to find the thermodynamic stability and kinetics of proteins unfolding. The monitoring of absorbance at 230 nm (A_{230}) during the heating was used as structural probe for studying apoferritin. The steady decrease of A_{230} was observed from 30 °C to 76 °C during the heating of apoferritin solution (Fig. 1J). The absorbance of apoferritin solution at 30 °C and 76 °C was expressed as 100% and 0%, respectively. The lowest absorbance (A_{230} = 1.28 AU) was measured after the temperature of the solution reached 76 °C; however, the absorbance of solutions heated to 68 °C and more were nearly the same. We suggest that the heating of apoferritin above the body temperature resulted in the conformation changes of the apoferritin subunits and total denaturation at 68 °C was observed; nevertheless, the substantial reversibility of horse spleen apoferritin denaturation was observed up to a few degrees below denaturation temperature.[11] The UV spectra of folded and unfolded protein commonly shows downward peak (UV absorption of unfolded protein is lower).[58]

The unfolding and denaturation of apoferritin were also examined using the native polyacrylamide gel electrophoresis (Fig. 1K). Smears corresponding to the release of apoferritin subunits were observed in case of samples heated above 65 °C but it seems to have reached a higher intensity at 70 °C. Taking together data from UV absorption and gel electrophoresis, we conclude that the spherical structure of apoferritin degrades in temperature above 65 °C. Based on previous results, we have chosen 60 °C as a safe temperature for CdTe NPs aggregation in the presence of the spherical state of apoferritin. Stefanini *et al.* (1996) suggests that the horse spleen apoferritin should not be heated to 80 °C to avoid its irreversible denaturation.[11] Our results confirm the high thermostability of horse spleen apoferritin, which is consistent with the thermostability of the entire ferritin group as it was determined in the case of ferritin from hyperthermophile *Pyrococcus furiosus*, which is stable up to 120 °C.[14]

The average particle sizes and particle size distribution within samples were determined using a zetasizer; nevertheless, electrochemical methods were suggested to be able to determine nanoparticle sizes (Fig. 1L).[59] Average CdTe colloid was 295 nm in diameter after heating, although we assume that their size without capping agent is not stable. The average size of spherical apoferritin was found to be 11 nm, which correspond with the commonly accepted size of apoferritin (12 nm). Two main particle fractions were detected in the case of ApoCdTe NPs sample as (i) CdTe colloids with average sizes of 255 nm and (ii) apoferritin modified by CdTe NPs with average diameter of 18 nm.

As we observed the quenching of CdTe NPs fluorescence by apoferritin and *vice versa*, we used the calculations of Stern–Volmers constants to elucidate the interaction of CdTe NPs and

apoferritin surface. Fluorescence quenching mechanism is usually described as either dynamic or static and can be determined using different temperature dependence.[60] As it is shown in Fig. 1M, the calculated Stern–Volmer quenching constants K_{SV} of CdTe NPs were inversely correlated with the increasing temperature. This phenomenon is often observed in the case of static quenching and suggests that the quenching of CdTe NPs was the result of them binding to the surface of apoferritin, rather than by dynamic collision.[61]

3.2. Anchoring of the apoferritin samples

The utilization of the apoferritin cage as a nanoreactor provides variety of advantages; however, the manipulation of such a molecule by external stimuli is of an interest mainly to enable the reaction to take place at the desired place, and subsequently transfer the product to the site of action. Therefore, an elegant approach of application of magnetic particles can be used. For this reason, a simple connection using gold nanoparticles and complementary oligonucleotides was proposed, enabling to simply connect the cage to the magnetic particle and spatially manipulate the nanoreactor.

In the following experiments, apoferritin, CdTe NPs and ApoCdTe NPs samples were mixed with the gold nanoparticles (Au NPs). Covalent bond between Au and S is the most widely used interaction to achieve stable conjugation between Au NPs and oligonucleotides or proteins containing cysteine.[62–64] The citrate capped Au NPs are known as one of the easily synthesized NPs, thus are frequently used for biosensors fabrication and biomolecule labelling.[65–67] The exposed citrate is responsible for the negative charge of Au NPs surface.[68] Due to the fact that the apoferritin inner surface has a negative electrostatic potential due to the presence of many acidic amino acids residues, which is important to attract metal ions from solution during biomineralization, the electrostatic binding between Au NPs and apoferritin (horse spleen apoferritin p*I* is between 4.1–5.5) is impossible in neutral pH.[69] Our concept of apoferritin modification with Au NPs relies on the apoferritin's ability to displace the citrate on nanoparticle surface as a result of the direct interaction of amino acids functional group (thiol of cysteine, amine of lysine or imidazole of histidine) with the gold surface. The forming of chemical bond between sulphur from apoferritin cysteine and gold was previously reported.[70]

The integrity of apoferritin structure during the CdTe NPs synthesis was examined using gel electrophoresis (Fig. 2A). The apoferritin sample and apoferritin sample after Au NPs modification was run in the gel (Fig. 2Aa and e). The band of native apoferritin nanosphere was found to be app. 1 cm from the beginning (Fig. 2A red arrow), which was reported by Kilic *et al.* under these conditions.[71] The faint band attributed to the dimeric form of apoferritin sphere was also observed (Fig. 2A green arrow), which was in good agreement with Kilic *et al.*[36] After apoferritin sample heating (20 h, 60 °C, 500 rpm), the sample was filtered using filter unit with 50 kDa cut off and the filtrate was analysed on PAGE (Fig. 2Ac). There was no apoferritin subunit band detected (both approximately 20 kDa), thus we concluded that the integration of apoferritin was mostly preserved after heating. The ApoCdTe NPs sample was treated in the same way. In Fig. 2Ab, d and f shows the ApoCdTe NPs sample after synthesis and its filtrate and ApoCdTe NPs modified by Au NPs. The positions of ApoCdTe NPs sample bands were similar to bands of apoferritin sample. Only slight shifts of ApoCdTe NPs bands were observed. We assume that the protein charge was not changed. Therefore, we came to the conclusion that it was the result of CdTe NPs attachment to the apoferritin surface and the increase of its hydrodynamic size, as also suggested by the particles size distribution and static quenching of CdTe NPs fluorescence by apoferritin (Fig. 1L).

In conclusion, no shifts of the bands of apoferritin and ApoCdTe NPs were observed after their modification with gold

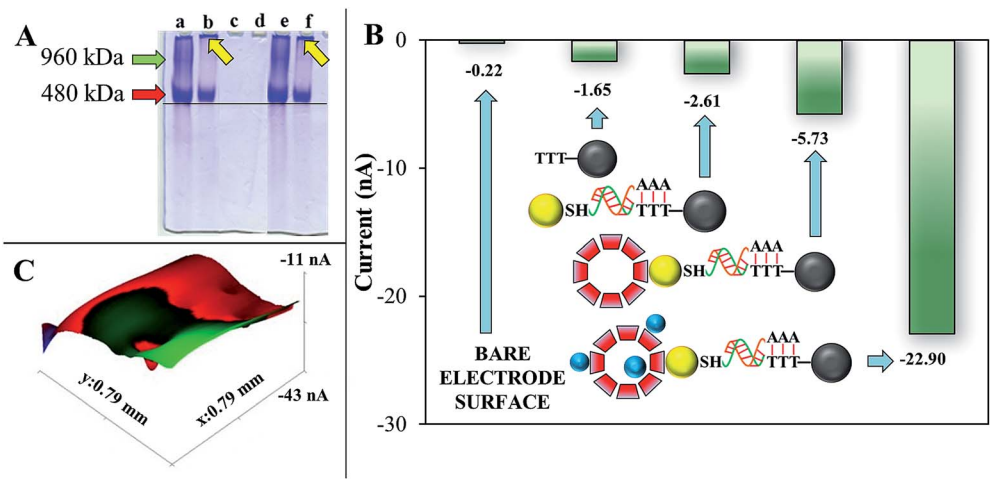

Fig. 2 Creation of anchor system. (A) The native PAGE shows the (a) apoferritin sample, (b) the ApoCdTe NPs sample after heating, (c and d) the filtrate obtained by filtration of apoferritin and ApoCdTe NPs sample through filter unit after heating, and (e and f) apoferritin and ApoCdTe NPs sample after Au NPs modification. (B) The average current levels of individual parts of nanoconstruct measured by SECM confirmed individual steps of anchor system creation. (C) The image of ApoCdTe NPs anchored to magnetic particles obtained by SECM.

nanoparticles. The bands intensities of ApoCdTe NPs and ApoCdTe NPs modified with Au NPs were not so well-marked as the apoferritin bands. The thermostability of apoferritin seems to be partly influenced by CdTe NPs presence. Heating (60 °C for 20 h) resulted in apoferritin portion unfolding, indicated by polypeptide aggregates, which cannot go through the native-PAGE and for this reason stacked at the beginning of the gel (Fig. 2A yellow arrow) and they were also not able to go through the filter unit with 50 kDa cut-off.

The individual steps of nanoconstruct formation were examined using SECM (Fig. 2B). The bare gold plate was first scanned and the average current level was calculated (−0.22 nA). The magnetic particles attached to the gold plate due to magnetic field had an average current level of −1.65 nA. The oligonucleotide with terminal polyA sequence was hybridized to magnetic particles. This complex was then hybridized to complementary oligonucleotide with thiolated terminus and Au NPs were immobilized on its thiol groups. This part of construct decreased the reduction signal by 0.96 nA to −2.61 nA. The construct extended by apoferritin resulted in the decrease of the signal by 3.12 nA to −5.73 nA, therefore the apoferritin addition increased the amount of reducible substances by 120%. The presence of CdTe NPs within the apoferritin cavity and on the apoferritin surface decreased the average current level four-times to −22.90 nA. The SECM record of ApoCdTe NPs immobilized on the surface of gold electrode using anchor system and applying of external magnetic field is shown in Fig. 2C.

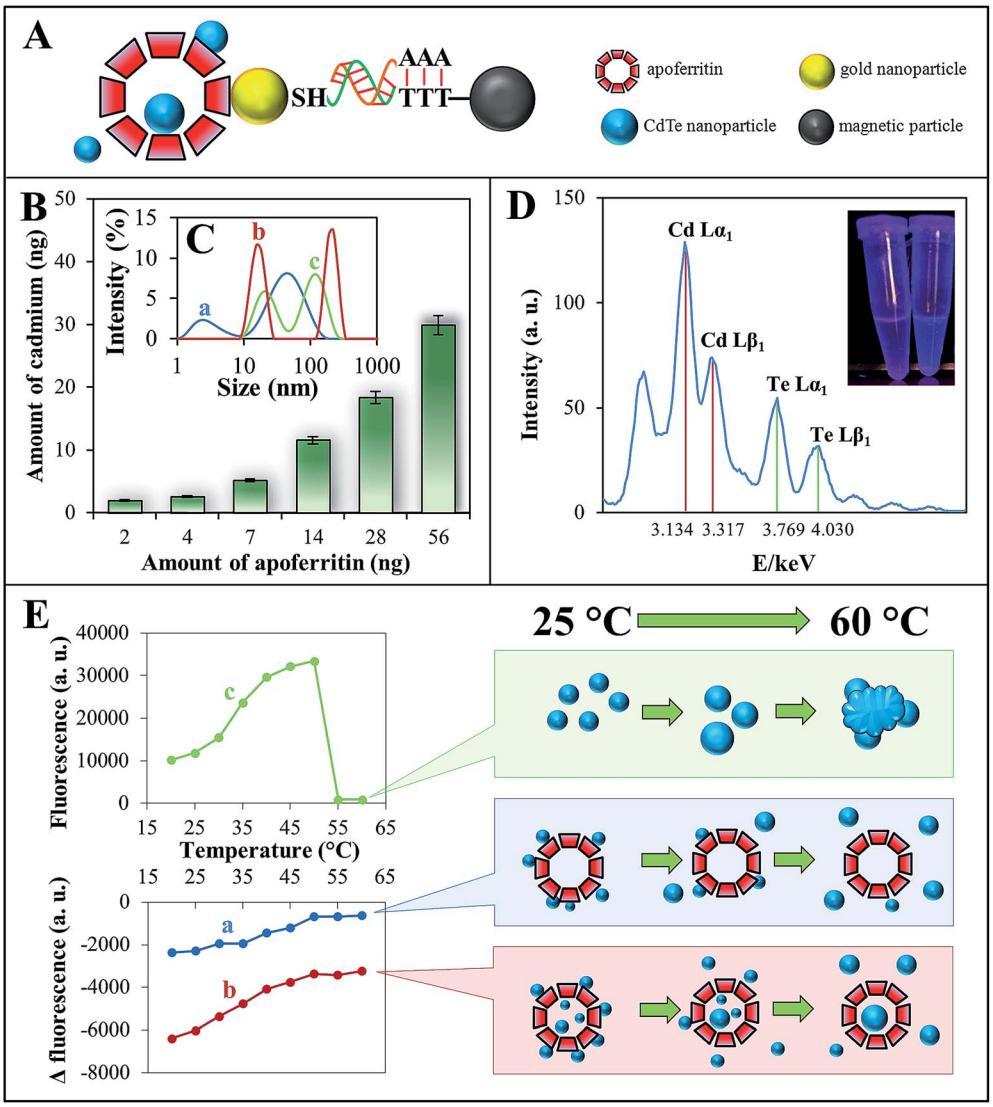

Fig. 3 Proving of apoferritin modification with CdTe NPs. (A) The scheme of ApoCdTe NPs anchored to the separative nanoconstruct used to prove the dependence of the detected cadmium amount on the amount of anchored apoferritin (B). (C) The sizes of gold nanoparticles (a) used for apoferritin modification, (b) particles presented within the ApoCdTe NPs sample and (c) the particles separated by anchor system. (D) The XRF spectra shows that Cd and Te ions were presented in ApoCdTe NPs sample separated by the anchor system. Inset: the image of water on the left and ApoCdTe NPs on the right side after excitation by 312 nm. (E) The dependence of fluorescence on the heating temperature for (a) CdTe solution with apoferritin added after CdTe synthesis, (b) ApoCdTe NPs and (c) the CdTe without any capping agent suggests that portion of CdTe NPs is presented within apoferritin cavity.

3.3. The presence of CdTe nanoparticles within apoferritin

The Au NPs were added to apoferritin, CdTe NPs and ApoCdTe NPs samples. After incubation of the samples with the Au NPs, we used the anchor system to capture the Au NPs and molecules attached to them (Fig. 3A). Oligonucleotide probes with terminal AAA sequence were hybridized to magnetic particles with TTT sequence bound to theirs surface. Second probes with thiol groups were hybridized to the first one and together formed a system capable of anchoring gold modified biomolecules. The different concentrations of ApoCdTe NPs sample modified with Au NPs were added to oligonucleotides with attached magnetic particles. CdTe NPs solution was added to the magnetic particle as a control. After incubation (1 h, 25 °C), these constructs were separated from the solution of unattached molecules by applying external magnetic field. Subsequently, the hybridized oligonucleotides in the constructs were disrupted due to chemical denaturation and the magnetic particles were removed from the samples. Finally, the samples were analysed using AAS. No trace of cadmium was detected in the control samples. It means that no CdTe NPs were modified by Au NPs and anchored. Apart from that, ApoCdTe NPs was successfully modified by Au NPs and attached to the anchor system. The dependence of detected amount of total cadmium on the volume of ApoCdTe NPs applied to the anchor system proved the modification of apoferritin by CdTe NPs and it is shown in Fig. 3B. Furthermore, we calculated that the ratio of the detected cadmium to one apoferritin anchored molecule to be 2700 : 1. The sizes and size distributions of gold nanoparticles used for apoferritin modification and particles separated from ApoCdTe NPs solution were measured and compared with the size distribution of the particles presented within the ApoCdTe NPs solution (Fig. 3C). We observed that gold nanoparticles with average diameter of 4 nm exhibited a broad size distribution from 1 to 8 nm. In this case, we suggested that the gold nanoparticles aggregation and cluster formation was partly responsible for this size distribution and also for the presence of second size distribution peak from 10 to 120 nm. The size distribution of ApoCdTe NPs sample consisted of two peaks. The first peak, at app. 18 nm, was assigned to the apoferritin with CdTe NPs present on its surface and the second to the CdTe colloids with sizes from 165 to 340 nm. The size distribution of particles separated from the ApoCdTe NPs solution by anchor system shows that the apoferritin was modified by Au NPs and probably also attached to the Au NPs clusters. The size distribution of particles attributed to apoferritin modified with CdTe NPs and Au NPs was from 12 to 42 nm with the biggest intensity at 21 nm. We assume that the thiolated oligonucleotide was still bound to the apoferritin and contributed to the peak shift. Particles with size of 105 nm were also separated from ApoCdTe NPs solution, which suggests that the aggregated Au NPs were also anchored. Although the small overlap of CdTe NPs colloids size distribution from ApoCdTe NPs sample and size distribution of particles separated from ApoCdTe NPs sample was observed, we concluded that no CdTe NPs colloids were anchored, because no fraction bigger than CdTe NPs colloids was observed in the size distribution of the anchored particles, which confirms the results from AAS measurement of the control sample. The sample, where the highest concentration of cadmium was proven, was also analysed by X-ray fluorescence (XRF). The measurement of XRF spectra confirmed the presence of tellurium (the $L\alpha_1$ line energy corresponds to 3.134 keV and $L\beta_1$ to 3.317 keV) and also cadmium (the $L\alpha_1$ corresponds to 3.769 keV and $L\beta_1$ to 4.030 keV) in the solution containing ApoCdTe NPs (Fig. 3D).

We also tested the effect of CdTe NPs nanoparticles on the fluorescence of tryptophan in apoferritin. The fluorescence spectra of ApoCdTe NPs sample were compared with the spectra of CdTe NPs solution with added apoferritin. Apoferritin emissions in the presence of cadmium, tellurite and ammonium ions were measured and subtracted from the emissions of ApoCdTe NPs and the mixture of CdTe NPs and apoferritin, which were monitored during heating (20, 25, 30, 35, 40, 45, 50, 55 and 60 °C) using an excitation wavelength of 380 nm. This excitation wavelength was chosen in order to observe changes in the apoferritin emission peak width rather than emission maxima and to enable observing the subtle changes of tryptophan fluorescence. The addition of apoferritin to CdTe NPs solution resulted in the complete disappearance of CdTe NPs peak at 602 nm, which was replaced by the emission of tryptophan at 450 nm (excitation wavelength 380 nm). The concentration dependent ability of protein to quench different types CdTe quantum dots was previously described by Wang *et al.*[72] and the mechanism of apoferritin interaction with CdTe NPs without surface stabilisation was described by Stern–Volmer equation described above. In addition, we compared the fluorescence intensities of ApoCdTe NPs and apoferritin covered with CdTe NPs. In the case of both the samples, the fluorescence of apoferritin tryptophan was statically quenched (fluorescence was decreased) by the presence of CdTe NPs on apoferritin surface, whereas it was reported previously that hydrous ferric oxides emerging at ferroxidase centres are able to quench tryptophan fluorescence.[73] The increasing temperatures resulted in the growing and, finally, aggregation of CdTe NPs, which is in good agreement with results obtained by Shen *et al.*[74] It also induced release of growing CdTe NPs from apoferritin surface and led to the increase of apoferritin fluorescence (Fig. 3E). The total release was observed at 50 °C. After the release of CdTe NPs from apoferritin surface, the fluorescence of apoferritin with CdTe NPs within the cavity was still partly quenched (Fig. 3Eb). On the contrary, the fluorescence of apoferritin with CdTe only on its surface was almost same as apoferritin control after heating.

4. Conclusions

Apoferritin is an appealing molecule due to its inner cavity, and is extensively investigated as a nanoreactor or drug carrier. We designed the nanoconstruct, which is able to selectively bind apoferritin molecules modified by gold nanoparticles and separate them from the solution of unreacted components and therefore to purify the required product. This simple anchor system enables to analyse the anchored molecule modification

with the target analyte, also its degree or amount of encapsulated analyte. In order to test this concept we utilized apoferritin cavity as a nanoreactor and synthesized apoferritin modified by CdTe nanoparticles, which proved to be presented on the surface and within the apoferritin cavity.

Acknowledgements

The financial support from the following project NANOLABSYS CZ.1.07/2.3.00/20.0148 is highly acknowledged. The authors thank Dagmar Uhlirova, Martina Stankova and Radek Chmela for technical assistance.

References

1 G. M. Whitesides, *Small*, 2005, **1**, 172–179.
2 L. Sironi, S. Freddi, M. Caccia, P. Pozzi, L. Rossetti, P. Pallavicini, A. Dona, E. Cabrini, M. Gualtieri, I. Rivolta, A. Panariti, L. D'Alfonso, M. Collini and G. Chirico, *J. Phys. Chem. C*, 2012, **116**, 18407–18418.
3 B. S. Yin, S. W. Zhang, Y. Jiao, Y. Liu, F. Y. Qu, Y. J. Ma and X. Wu, *J. Nanosci. Nanotechnol.*, 2014, **14**, 7157–7160.
4 H. Zhang, S. S. Jia, M. Lv, J. Y. Shi, X. L. Zuo, S. Su, L. H. Wang, W. Huang, C. H. Fan and Q. Huang, *Anal. Chem.*, 2014, **86**, 4047–4051.
5 G. D. Liu, H. Wu, J. Wang and Y. H. Lin, *Small*, 2006, **2**, 1139–1143.
6 H. L. Li, Y. C. Zhu, S. G. Chen, O. Palchik, J. P. Xiong, Y. Koltypin, Y. Gofer and A. Gedanken, *J. Solid State Chem.*, 2003, **172**, 102–110.
7 H. Y. Hsueh, H. Y. Chen, Y. C. Hung, Y. C. Ling, S. Gwo and R. M. Ho, *Adv. Mater.*, 2013, **25**, 1780–1786.
8 W. Zhou, K. Zheng, L. He, R. M. Wang, L. Guo, C. P. Chen, X. Han and Z. Zhang, *Nano Lett.*, 2008, **8**, 1147–1152.
9 K. Uto, K. Yamamoto, N. Kishimoto, M. Muraoka, T. Aoyagi and I. Yamashita, *J. Nanosci. Nanotechnol.*, 2014, **14**, 3193–3201.
10 C. B. Mao, D. J. Solis, B. D. Reiss, S. T. Kottmann, R. Y. Sweeney, A. Hayhurst, G. Georgiou, B. Iverson and A. M. Belcher, *Science*, 2004, **303**, 213–217.
11 S. Stefanini, S. Cavallo, C. Q. Wang, P. Tataseo, P. Vecchini, A. Giartosio and E. Chiancone, *Arch. Biochem. Biophys.*, 1996, **325**, 58–64.
12 R. R. Crichton and C. F. A. Bryce, *Biochem. J.*, 1973, **133**, 289–299.
13 M. Uchida, M. T. Klem, M. Allen, P. Suci, M. Flenniken, E. Gillitzer, Z. Varpness, L. O. Liepold, M. Young and T. Douglas, *Adv. Mater.*, 2007, **19**, 1025–1042.
14 M. J. Parker, M. A. Allen, B. Ramsay, M. T. Klem, M. Young and T. Douglas, *Chem. Mater.*, 2008, **20**, 1541–1547.
15 I. Yamashita, J. Hayashi and M. Hara, *Chem. Lett.*, 2004, **33**, 1158–1159.
16 T. Ueno, M. Suzuki, T. Goto, T. Matsumoto, K. Nagayama and Y. Watanabe, *Angew. Chem., Int. Ed.*, 2004, **43**, 2527–2530.
17 R. Tsukamoto, K. Iwahori, M. Muraoka and I. Yamashita, *Abstr. Pap. Am. Chem. Soc.*, 2005, **229**, U938–U939.
18 B. Hennequin, L. Turyanska, T. Ben, A. M. Beltran, S. I. Molina, M. Li, S. Mann, A. Patane and N. R. Thomas, *Adv. Mater.*, 2008, **20**, 3592–3596.
19 T. D. Bradshaw, M. Junor, A. Patane, P. Clarke, N. R. Thomas, M. Li, S. Mann and L. Turyanska, *J. Mater. Chem. B*, 2013, **1**, 6254–6260.
20 X. Y. Liu, W. Wei, S. J. Huang, S. S. Lin, X. Zhang, C. M. Zhang, Y. G. Du, G. H. Ma, M. Li, S. Mann and D. Ma, *J. Mater. Chem. B*, 2013, **1**, 3136–3143.
21 K. L. Fan, L. Z. Gao and X. Y. Yan, *Wiley Interdiscip. Rev.: Nanomed. Nanobiotechnol.*, 2013, **5**, 287–298.
22 E. Fantechi, C. Innocenti, M. Zanardelli, M. Fittipaldi, E. Falvo, M. Carbo, V. Shullani, L. D. Mannelli, C. Ghelardini, A. M. Ferretti, A. Ponti, C. Sangregorio and P. Ceci, *ACS Nano*, 2014, **8**, 4705–4719.
23 I. Blazkova, H. V. Nguyen, S. Dostalova, P. Kopel, M. Stanisavljevic, M. Vaculovicova, M. Stiborova, T. Eckschlager, R. Kizek and V. Adam, *Int. J. Mol. Sci.*, 2013, **14**, 13391–13402.
24 B. H. Jun, M. S. Noh, G. Kim, H. Kang, J. H. Kim, W. J. Chung, M. S. Kim, Y. K. Kim, M. H. Cho, D. H. Jeong and Y. S. Lee, *Anal. Biochem.*, 2009, **391**, 24–30.
25 D. Huska, J. Hubalek, V. Adam, D. Vajtr, A. Horna, L. Trnkova, L. Havel and R. Kizek, *Talanta*, 2009, **79**, 402–411.
26 J. H. Min, M. K. Woo, H. Y. Yoon, J. W. Jang, J. H. Wu, C. S. Lim and Y. K. Kim, *Anal. Biochem.*, 2014, **447**, 114–118.
27 S. H. Lim, F. Bestvater, P. Buchy, S. Mardy and A. D. C. Yu, *Sensors*, 2009, **9**, 5590–5599.
28 L. B. Nie, X. L. Wang, S. Li and H. Chen, *Anal. Sci.*, 2009, **25**, 1327–1331.
29 F. Patolsky, Y. Weizmann, E. Katz and I. Willner, *Angew. Chem., Int. Ed.*, 2003, **42**, 2372–2376.
30 Y. S. Xing, P. Wang, Y. C. Zang, Y. Q. Ge, Q. H. Jin, J. L. Zhao, X. Xu, G. Q. Zhao and H. J. Mao, *Analyst*, 2013, **138**, 3457–3462.
31 C. L. Cowles and X. S. Zhu, *Anal. Methods*, 2013, **5**, 801–804.
32 P. Hu, C. Z. Huang, Y. F. Li, J. Ling, Y. L. Liu, L. R. Fei and J. P. Xie, *Anal. Chem.*, 2008, **80**, 1819–1823.
33 X. L. Han, P. Mei, Y. Liu, Q. Xiao, F. L. Jiang and R. Li, *Spectrochim. Acta, Part A*, 2009, **74**, 781–787.
34 J. Kimling, M. Maier, B. Okenve, V. Kotaidis, H. Ballot and A. Plech, *J. Phys. Chem. B*, 2006, **110**, 15700–15707.
35 J. Polte, T. T. Ahner, F. Delissen, S. Sokolov, F. Emmerling, A. F. Thunemann and R. Kraehnert, *J. Am. Chem. Soc.*, 2010, **132**, 1296–1301.
36 M. A. Kilic, S. Spiro and G. R. Moore, *Protein Sci.*, 2003, **12**, 1663–1674.
37 J. R. Lakowicz, *Principles of Fluorescence Spectroscopy*, Springer, New York, 2006.
38 Q. Xiao, H. N. Qiu, S. Huang, C. S. Huang, W. Su, B. Q. Hu and Y. Liu, *Mol. Biol. Rep.*, 2013, **40**, 5781–5789.
39 T. Takahashi and S. Kuyucak, *Biophys. J.*, 2003, **84**, 2256–2263.
40 S. Aime, L. Frullano and S. G. Crich, *Angew. Chem., Int. Ed.*, 2002, **41**, 1017–1019.

41 K. Bartling, A. Sambanis and R. W. Rousseau, *Cryst. Growth Des.*, 2007, **7**, 569–575.
42 D. M. Lawson, P. J. Artymiuk, S. J. Yewdall, J. M. A. Smith, J. C. Livingstone, A. Treffry, A. Luzzago, S. Levi, P. Arosio, G. Cesareni, C. D. Thomas, W. V. Shaw and P. M. Harrison, *Nature*, 1991, **349**, 541–544.
43 A. Datta, S. Chatterjee, A. K. Sinha, S. N. Bhattacharyya and A. Saha, *J. Lumin.*, 2006, **121**, 553–560.
44 J. T. Vivian and P. R. Callis, *Biophys. J.*, 2001, **80**, 2093–2109.
45 A. Kowalska-Baron, K. Galecki, K. Rozniakowski, B. Kolesinska, Z. J. Kaminski and S. Wysocki, *Spectrochim. Acta, Part A*, 2014, **128**, 830–837.
46 I. Yamashita, *Abstr. Pap. Am. Chem. Soc.*, 2005, **229**, U906.
47 H. Y. Han, Z. H. Sheng and H. G. Liang, *Mater. Lett.*, 2006, **60**, 3782–3785.
48 Y. Khalavka, B. Mingler, G. Friedbacher, G. Okrepka, L. Shcherbak and O. Panchuk, *Phys. Status Solidi A*, 2010, **207**, 370–374.
49 K. K. W. Wong and S. Mann, *Adv. Mater.*, 1996, **8**, 928.
50 J. B. Xiao, Y. L. Bai, Y. F. Wang, J. W. Chen and X. L. Wei, *Spectrochim. Acta, Part A*, 2010, **76**, 93–97.
51 J. Zhang, L. N. Chen, B. R. Zeng, Q. L. Kang and L. Z. Dai, *Spectrochim. Acta, Part A*, 2013, **105**, 74–79.
52 H. Herberhold, S. Marchal, R. Lange, C. H. Scheyhing, R. F. Vogel and R. Winter, *J. Mol. Biol.*, 2003, **330**, 1153–1164.
53 D. W. Yang, K. Matsubara, M. Yamaki, S. Ebina and K. Nagayama, *Biochim. Biophys. Acta, Protein Struct. Mol. Enzymol.*, 1994, **1206**, 173–179.
54 M. Weik and J. P. Colletier, *Acta Crystallogr., Sect. D: Biol. Crystallogr.*, 2010, **66**, 437–446.
55 H. Wu, S. H. Fan, H. Chen, J. Shen, Y. Y. Geng, L. Peng and H. L. Du, *Anal. Methods*, 2014, **6**, 4729–4733.
56 Z. Kriz, J. Klusak, Z. Kristofikova and J. Koca, *PLoS One*, 2013, **8**, 1–14.
57 R. Esfandiary, J. S. Hunjan, G. H. Lushington, S. B. Joshi and C. R. Middaugh, *Protein Sci.*, 2009, **18**, 2603–2614.
58 P. F. Liu, L. V. Avramova and C. Park, *Anal. Biochem.*, 2009, **389**, 165–170.
59 M. Giovanni and M. Pumera, *Electroanalysis*, 2012, **24**, 615–617.
60 Y. J. Hu, C. H. Chen, S. Zhou, A. M. Bai and Y. Ou-Yang, *Mol. Biol. Rep.*, 2012, **39**, 2781–2787.
61 M. Hossain, A. Y. Khan and G. S. Kumar, *PLoS One*, 2011, **6**, 1–12.
62 F. Li, H. Q. Zhang, B. Dever, X. F. Li and X. C. Le, *Bioconjugate Chem.*, 2013, **24**, 1790–1797.
63 B. L. V. Prasad, C. M. Sorensen and K. J. Klabunde, *Chem. Soc. Rev.*, 2008, **37**, 1871–1883.
64 A. Vallee, V. Humblot and C. M. Pradier, *Acc. Chem. Res.*, 2010, **43**, 1297–1306.
65 F. Y. Yeh, T. Y. Liu, I. H. Tseng, C. W. Yang, L. C. Lu and C. S. Lin, *Biosens. Bioelectron.*, 2014, **61**, 336–343.
66 R. Luo, Y. H. Li, X. J. Lin, F. Dong, W. Zhang, L. Yan, W. Cheng, H. X. Ju and S. J. Ding, *Sens. Actuators, B*, 2014, **198**, 87–93.
67 M. Pumera, M. Aldavert, C. Mills, A. Merkoci and S. Alegret, *Electrochim. Acta*, 2005, **50**, 3702–3707.
68 G. Tomoaia, P. T. Frangopol, O. Horovitz, L. D. Bobos, A. Mocanu and M. Tomoaia-Cotisel, *J. Nanosci. Nanotechnol.*, 2011, **11**, 7762–7770.
69 P. Arosio, T. G. Adelman and J. W. Drysdale, *J. Biol. Chem.*, 1978, **253**, 4451–4458.
70 J. W. Kim, A. E. Posey, G. D. Watt, S. H. Choi and P. T. Lillehei, *J. Nanosci. Nanotechnol.*, 2010, **10**, 1771–1777.
71 M. A. Kilic, E. Ozlu and S. Calis, *J. Biomed. Nanotechnol.*, 2012, **8**, 508–514.
72 S. S. Wang, X. T. Wang, M. M. Guo and J. S. Yu, *Chem. J. Chin. Univ.*, 2012, **33**, 1195–1204.
73 F. Bou-Abdallah, G. Zhao, G. Biasiotto, M. Poli, P. Arosio and N. D. Chasteen, *J. Am. Chem. Soc.*, 2008, **130**, 17801–17811.
74 M. Shen, W. P. Jia, Y. J. You, Y. Hu, F. Li, S. D. Tian, J. Li, Y. X. Jin and D. M. Han, *Nanoscale Res. Lett.*, 2013, **8**, 1–6.

